

## Article (refereed) - postprint

---

Riddick, S.N.; Blackall, T.D.; Dragosits, U.; Daunt, F.; Braban, C.F.; Tang, Y.S.; MacFarlane, W.; Taylor, S.; Wanless, S.; Sutton, M.A.. 2014.

### **Measurement of ammonia emissions from tropical seabird colonies.**

Copyright © 2014 Elsevier B.V.

This version available <http://nora.nerc.ac.uk/506785/>

NERC has developed NORA to enable users to access research outputs wholly or partially funded by NERC. Copyright and other rights for material on this site are retained by the rights owners. Users should read the terms and conditions of use of this material at

<http://nora.nerc.ac.uk/policies.html#access>

NOTICE: this is the author's version of a work that was accepted for publication in *Atmospheric Environment*. Changes resulting from the publishing process, such as peer review, editing, corrections, structural formatting, and other quality control mechanisms may not be reflected in this document. Changes may have been made to this work since it was submitted for publication. A definitive version was subsequently published in *Atmospheric Environment*, 89. 35-42. [10.1016/j.atmosenv.2014.02.012](https://doi.org/10.1016/j.atmosenv.2014.02.012)

[www.elsevier.com/](http://www.elsevier.com/)

Contact CEH NORA team at  
[noraceh@ceh.ac.uk](mailto:noraceh@ceh.ac.uk)

# 1 Measurement of ammonia emissions from tropical seabird colonies

2 S. N. Riddick<sup>1, 2, 3, 4</sup>, T. D. Blackall<sup>1</sup>, U. Dragosits<sup>2</sup>, F. Daunt<sup>2</sup>, C. F. Braban<sup>2</sup>, Y. S.  
3 Tang<sup>2</sup>, W. MacFarlane<sup>5, 6</sup>, S. Taylor<sup>5</sup>, S. Wanless<sup>2</sup> and M. A. Sutton<sup>2</sup>

4 <sup>1</sup> King's College London, Strand, London, UK

5 <sup>2</sup> Centre for Ecology & Hydrology Edinburgh, Bush Estate, Midlothian, EH26 0QB

6 <sup>3</sup> Cornell University, Ithaca, NY, USA

7 <sup>4</sup> Now at Department of Chemistry, University of Cambridge, UK

8 <sup>5</sup> Queensland Parks and Wildlife Service (Marine Parks), Queensland Department of  
9 National Parks, Recreation, Sports and Racing, Brisbane, Australia

10 <sup>6</sup> Now at JWM Marine Consultancy, Cairns, Australia

11 Contact: S. Riddick, Tel: 01223 763823, email: sr694@cam.ac.uk

12 **Key Words:** Coastal nitrogen; seabirds; NH<sub>3</sub> measurement; atmospheric dispersion  
13 modelling

## 14 Abstract

15 The excreta (guano) of seabirds at their breeding colonies represents a notable source  
16 of ammonia (NH<sub>3</sub>) emission to the atmosphere, with effects on surrounding  
17 ecosystems through nitrogen compounds being thereby transported from sea to land.  
18 Previous measurements in temperate UK conditions quantified emission hotspots and  
19 allowed preliminary global upscaling. However, thermodynamic processes and water  
20 availability limit NH<sub>3</sub> formation from guano, which suggests that the proportion of  
21 excreted nitrogen that volatilizes as NH<sub>3</sub> may potentially be higher at tropical seabird  
22 colonies than similar colonies in temperate or sub-polar regions. To investigate such  
23 differences, we measured NH<sub>3</sub> concentrations and environmental conditions at two  
24 tropical seabird colonies during the breeding season: a colony of 20,000 tern *spp.* and  
25 noddies on Michaelmas Cay, Great Barrier Reef, and a colony of 200,000 Sooty terns  
26 on Ascension Island, Atlantic Ocean. At both sites time-integrated NH<sub>3</sub>  
27 concentrations and meteorological parameters were measured. In addition, at  
28 Ascension Island, semi-continuous hourly NH<sub>3</sub> concentrations and  
29 micrometeorological parameters were measured throughout the campaign. Ammonia  
30 emissions, quantified using a backwards Lagrangian atmospheric dispersion model,  
31 were estimated at 21.8 μg m<sup>-2</sup> s<sup>-1</sup> and 18.9 μg m<sup>-2</sup> s<sup>-1</sup> from Michaelmas Cay and  
32 Ascension Island, respectively. High temporal resolution NH<sub>3</sub> data at Ascension  
33 Island estimated peak hourly emissions up to 377 μg NH<sub>3</sub> m<sup>2</sup> s<sup>-1</sup>. The estimated  
34 percentage fraction of total guano nitrogen volatilized was 67% at Michaelmas Cay  
35 and 32% at Ascension Island, with the larger value at the former site attributed to  
36 higher water availability. These values are much larger than published data for sub-  
37 polar locations, pointing to a substantial climatic dependence on emission of  
38 atmospheric NH<sub>3</sub> from seabird colonies.

## 39 1. Introduction

40 Seabird colonies represent major point sources of ammonia (NH<sub>3</sub>) emissions to the  
41 atmosphere. Seabirds are globally distributed; therefore the NH<sub>3</sub> emissions occur in a  
42 wide range of climatic environments. The high nitrogen (N) diet of seabirds is almost  
43 exclusively marine-derived (Phillips et al., 1999) and excretal N mainly occurs in the  
44 form of uric acid. Through bacterial hydrolysis, the reaction product NH<sub>3</sub> is formed

45 (Wright, 1995) which is liable to volatilize to the atmosphere, disperse and be  
46 deposited to terrestrial ecosystems. The result is that seabird-derived  $\text{NH}_3$  provides a  
47 vector for transfer of marine N back to land (Blackall et al., 2008).

48 The majority of seabird colonies are found in remote coastal areas (e.g. Wilson et al.  
49 2004). Due to their isolation from anthropogenic reactive nitrogen ( $\text{N}_r$ ) sources,  
50 several studies suggest that seabird colonies are the most important pathway for plant  
51 nutrient supply within these ecosystems (Lindeboom, 1984; Hop et al., 2002).  
52 Schmidt et al. (2010) made measurements of  $\text{NH}_3$  concentrations and enzyme assays  
53 at a tropical coral cay with large bird colonies, and the results showed that the  
54 dominant source of vegetation N was foliar  $\text{NH}_3$  uptake.

55 In naturally low-N terrestrial ecosystems, even relatively small inputs of N from  
56 seabirds have been shown to cause increases in plant productivity that would not have  
57 normally been observed in already nutrient rich environments (Ellis, 2005). Even  
58 though N is essential for plant growth, excess  $\text{NH}_3$  can negatively affect tolerance to  
59 drought or frost and resistance to disease and insects in plants, and/or lead to long  
60 term changes in plant species composition, with nitrophilic plants out-competing  
61 species adapted to low-N environments (Cape et al., 2009; Sutton et al., 2011).

62 Ammonia emission data from seabird populations in contrasting weather conditions  
63 have not been previously reported and emission dynamics coupled to changes in  
64 weather are not well understood. Blackall et al. (2004, 2007) measured  $\text{NH}_3$   
65 concentrations downwind of UK (temperate weather conditions) seabird populations  
66 ( $T \sim 15^\circ\text{C}$  during the breeding season) and reported the percentage of seabird-N  
67 volatilized as  $\text{NH}_3$  ( $P_v$ ) = 33%. Environmental factors may have a significant impact  
68 on  $P_v$ , for example recent measurements by Theobald et al. (2013) suggest only 2%  
69  $\text{NH}_3$  volatilization of excreted penguin guano on mainland Antarctica.

70 The decomposition of uric acid to  $\text{NH}_3$  is temperature dependent (Elliott and Collins,  
71 1982), with decomposition increasing as temperature increases. Based on a scenario  
72 that  $P_v$  is highly thermodynamically dependent, Riddick et al. (2012) modelled  $P_v$   
73 normalized to the measurements of Blackall et al. (2007) and reaching  $\sim 100\%$  at  
74 tropical seabird colonies where the average temperature during the breeding season is  
75  $>19^\circ\text{C}$ . Several studies support the incorporation of thermodynamic dependences into  
76 land-atmosphere ecosystem exchange models for  $\text{NH}_3$  (e.g. Nemitz et al., 2001;  
77 Flechard et al., 2013). However, few studies have verified the extent of  
78 thermodynamic dependence.

79 In this work we present results from land-based measurements of  $\text{NH}_3$  concentrations  
80 and local meteorology at two seabird colonies in the tropics and use inverse-  
81 modelling to calculate the colony  $\text{NH}_3$  emissions and hence calculate  $P_v$  for each  
82 system. Continuous  $\text{NH}_3$  measurement data combined with micrometeorological  
83 measurement data were available for a four week campaign at Ascension Island  
84 (Atlantic Ocean), which was then matched temporally by passive  $\text{NH}_3$  measurements  
85 throughout the campaign. Comparison of the high-resolution  $\text{NH}_3$  concentrations (15  
86 minute) and micrometeorology measurements made on Ascension Island with parallel  
87 passive sampling measurements allowed the influence of sampling strategy to be  
88 assessed at Ascension. Secondly, the comparison of the passive sampling  
89 measurements at Ascension Island and Michaelmas Cay (Great Barrier Reef) allowed  
90 the influence of weather and local environment to be assessed.

## 91 **2. Methods and Materials**

## 92 2.1 Ammonia measurements

93 Ammonia concentration measurements were conducted using two methods: 1) time-  
94 integrated sampling (weekly to monthly) with passive diffusion samplers  
95 continuously sampling, and 2) continuous on-line ammonia analysis using a trace gas  
96 analyser. In the present study, the high sensitivity ALPHA (Adapted Low-cost  
97 Passive High Absorption) samplers were used with a MDL = 0.04  $\mu\text{g m}^{-3}$  for monthly  
98 exposure (Michaelmas Cay) and MDL = 0.19  $\mu\text{g m}^{-3}$  for weekly exposure (Ascension  
99 Island). A description of how the MDL was calculated is given in Supplementary  
100 Material Section 8.

101 Passive samplers have been widely used (e.g. Tang et al., 2001; Schmidt et al. 2010,  
102 Puchalski et al. 2011, Vogt et al. 2013) and performed well in a recent inter-  
103 comparison study of different passive samplers (Puchalski et al. 2011), though  
104 performance is dependent on the method variant and the details of its implementation  
105 (Sutton et al., 2001). In this study ALPHA samplers (Tang et al., 2001), were  
106 deployed in each field campaign in triplicate for the periods detailed below. They  
107 were attached with Velcro underneath shelters (upturned plant saucer) fixed on posts  
108 at measured heights above ground (as detailed in Section 2.2). To prevent false  
109 readings from contamination, spikes were mounted on top to deter bird perching and  
110 any disturbed samplers were not analysed. The samplers were stored in sealed plastic  
111 containers before and after exposure and, where possible, kept refrigerated. Citric acid  
112 coated filter papers from the samplers were extracted in 3 ml deionised water, and  
113 analysed for  $\text{NH}_4^+$  by flow injection analysis with conductivity detection (FLORRIA,  
114 Mechatronics, NL). Laboratory blanks were subtracted from samples and field blanks  
115 were used to check for contamination.

116 On-line continuous ammonia concentration measurements were made with an  
117 AiRRmonia gas analyser (Mechatronics, NL). The AiRRmonia analyser comprises a  
118 membrane sampler for quantitative sampling of gas-phase ammonia. After diffusion  
119 through the membrane, the ammonia is absorbed in a sampling solution which is  
120 pumped continuously. Ammonium ions pass through into a detector block *via*  
121 diffusion through an ion selective membrane. The ion concentration is measured with  
122 a conductivity detector. The AiRRmonia was housed in a weather-proof box and  
123 sampled air at 1  $\text{l}\cdot\text{min}^{-1}$  with a time resolution of ~15-20 minutes, dependent on  
124 relative humidity (RH). The instrument was operated with a heated Teflon inlet tube  
125 to prevent condensation and ensure a complete flow of  $\text{NH}_3$  through the tubing.  
126 Measurements were recorded every minute and the data then averaged for 15 minute  
127 periods. The AiRRmonia has a LOD of ~0.1  $\mu\text{g m}^{-3}$ , a MDL in this context of 0.07  $\mu\text{g}$   
128  $\text{m}^{-3}$  and has previously been used to measure  $\text{NH}_3$  emissions in agricultural field  
129 experiments (Norman et al. 2009). Calibration was carried out in the field every five  
130 days and showed good stability over the periods of measurement.

## 131 2.2 Field methodology

### 132 Site 1: Michaelmas Cay

133 Michaelmas Cay (16.60°S, 145.97°E) is a vegetated island cay within the Great  
134 Barrier Reef World Heritage Area off the east coast of Cairns, Australia. The  
135 Queensland Parks and Wildlife Service – Marine Parks (QPWS) conducted routine  
136 monthly bird counts. Measurements for this period indicate 20,000 seabirds breed on  
137 the island, including 3,000 Sooty terns (*Onychoprion fuscatus*), 9,000 Common  
138 noddies (*Anous stolidus*) and 1,500 Lesser-crested terns (*Thalasseus bengalensis*).

139 The island is hot and wet, with average air temperatures of 28°C and an average RH  
140 of 85%, as measured at Green Island, 10 km to the south (16.75°S, 145.97°E).

141 A passive NH<sub>3</sub> sampling campaign was conducted on Michaelmas Cay between  
142 November 2009 and January 2010. Four masts were set up with ALPHA samplers  
143 approximately 1 m above ground (Figure 1), with masts 1, 2 and 3 over the colony  
144 (Supplementary Material Section 1). It was intended that mast 4 should measure  
145 lower NH<sub>3</sub> concentrations (with no nesting birds present and located upwind relative  
146 to the prevailing wind direction). However, as this mast was <100 m from the bird  
147 colonies, NH<sub>3</sub> concentrations were still expected to be higher than background for an  
148 oceanic environment (e.g. NH<sub>3</sub> concentration of 0.01 µg m<sup>-3</sup>; Quinn et al., 1990).  
149 Sampling period 1 ran from 05/11/09 to 10/12/09 and sampling period 2 from  
150 10/12/09 to 06/01/10.

151 <<INSERT FIGURE 1>>

152 Ground temperature was measured using a Tinytag Talk 2 sensor (Gemini Data  
153 Loggers, UK). The sensor was attached to the mast on the surface of the sand to give  
154 a proxy of the surface temperature and recorded the temperature every three hours.  
155 Wind speed, wind direction, RH and precipitation for the measurement period were  
156 obtained from the meteorological station on Green Island, 10 km south of Michaelmas  
157 Cay. This represents the best meteorological data available for use in this study, as  
158 setting up an unattended meteorological station was discouraged due to the potential  
159 for interference by human visitors.

## 160 **Site 2: Ascension Island**

161 Ascension Island (7.99 °S, 14.39 °W) is a small volcanic island in the Atlantic Ocean.  
162 Ammonia concentrations and local meteorology were measured at the Sooty tern  
163 colony on the Wideawake Fairs in Mars Bay (Supplementary Material Section 2).  
164 *Circa* 100,000 pairs of Sooty tern were present during the measurements (N. Fowler,  
165 Conservation Department, Ascension Island, pers. comm.). The campaign used both  
166 continuous AiRRmonia and time-integrated ALPHA NH<sub>3</sub> measurements and was  
167 carried out between 22/05/2010 and 07/06/2010. The weather on Ascension Island is  
168 hot and dry with average air temperature during the breeding season at 2 m of 27°C,  
169 average humidity of 72% and average wind speed of 5 m s<sup>-1</sup> during the measurement  
170 period (meteorological data courtesy of the Met Office, Wideawake Airfield,  
171 Ascension Island).

172 ALPHA samplers were deployed and exposed for three periods: Period 1 (20/05/2010  
173 - 27/05/2010), Period 2 (27/05/2010 - 02/06/2010) and Period 3 (02/06/2010 -  
174 09/06/2010). During Periods 1 and 2, samplers were deployed at 4 locations (Figure  
175 2). Two extra samplers were added during Period 3 to provide more points on the  
176 concentration gradient away from the bird colony in the prevailing wind direction  
177 (Figure 2). In the first measurement period ALPHA samplers were located on Masts  
178 3, 4 and 5, the second period on Masts 1, 2 and 3 and in the third period ALPHAs  
179 were attached to all masts. The arrangements of the masts were changed between  
180 measurement periods to ensure NH<sub>3</sub> concentrations > LOD of the ALPHA samplers  
181 were measured. On all masts ALPHA samplers measured at 1.5 m above ground.  
182 This height was chosen to avoid contamination from the ground, also it was not too  
183 high to change the samplers. Background NH<sub>3</sub> concentrations were measured using  
184 ALPHA samplers 200 m upwind of the source area, which should provide an

185 indicative regional background, such as that measured by Norman and Leck (2005) at  
186  $0.36 \mu\text{g m}^{-3}$  for the central Atlantic Ocean.

187 <<INSERT FIGURE 2>>

188 The continuous AiRRmonia ( $\text{NH}_3$ ) measurements were made at a site downwind  
189 from the colony (labelled Met Station in Figure 2). The AiRRmonia was co-located  
190 with the meteorological measurement instrumentation. The sampling point was at a  
191 height of 2 m, with an inlet length of 10 m from inlet to detector. Due to the relatively  
192 high ambient temperatures and a heated inlet line, surface effects, though present,  
193 were minimised. The ammonia signal was corrected for transit through the inlet line  
194 and the inlet response to variations in ammonia concentrations was estimated to be  
195 short relative to the instrument response.

196 Meteorological measurements were made with standard met station equipment and a  
197 sonic anemometer as detailed in Supplementary Material Section 3. The spatial  
198 location of instruments and Sooty tern colony edge were mapped using a Garmin  
199 Etrex GPS (Garmin, Olathe, Kansas, USA), with an estimated accuracy of  $\pm 1.4$  m of  
200 true position in open sky settings (Wing et al., 2005).

## 201 **2.2 Calculation of $\text{NH}_3$ Emissions**

202 At both field sites the WindTrax atmospheric dispersion model (Flesch et al., 1995)  
203 was used to calculate the  $\text{NH}_3$  emission fluxes. On Ascension Island, where  
204 continuous  $\text{NH}_3$  data were available from the AiRRmonia measurements, both the  
205  $\text{NH}_3$  concentration and meteorological data were averaged over 15 minutes. This  
206 time period was used to match both the response time of the AiRRmonia and the time  
207 resolution recommended to minimise variability caused by turbulence, while  
208 including variation caused by environmental or atmospheric change (Laubach et al.  
209 2008).

210 Data were filtered for: calibration periods, periods when the measurement location  
211 was not downwind of the colony and for periods of strong atmospheric stability ( $u <$   
212  $0.15 \text{ ms}^{-1}$ ,  $u^* < 0.1 \text{ ms}^{-1}$  and  $|L| < 2$ ). Each simulation was run in WindTrax using  
213 50,000 particle projections to back-calculate the  $\text{NH}_3$  emission. Data input to  
214 WindTrax were 15 minute averages of: background  $\text{NH}_3$  concentrations ( $X_b$ ,  $\mu\text{g m}^{-3}$ ),  
215 wind speed ( $u$ ,  $\text{m s}^{-1}$ ), wind direction ( $WD$ ,  $^\circ$ ), temperature ( $T$ ,  $^\circ\text{C}$ ),  $\text{NH}_3$  concentration  
216 at 2 m ( $X$ ,  $\mu\text{g m}^{-3}$ ), roughness height ( $z_0$ , cm) and the Monin-Obukhov length ( $L$ , m).  
217 Emission estimates using the time-integrated version of the active sampling data in  
218 WindTrax used the same method as for the active sampling data

219 For both Ascension Island and Michaelmas Cay, the time-integrated passive  $\text{NH}_3$   
220 measurements were combined with the meteorological data to provide long-term  
221 estimates using the inverse dispersion model. In this way, an estimate of the  
222 uncertainties associated with the application of the inverse dispersion model when  
223 using time integrated passive sampling was assessed.

## 224 **2.3 Uncertainties**

225 In order to understand the uncertainties in the emission calculation, the input variables  
226 were assessed for both field sites. The uncertainty caused by each variable was  
227 estimated using simulations to back-calculate the change in  $\text{NH}_3$  emission. The total  
228 uncertainty was then calculated as the square root of the sum of the individual  
229 uncertainties squared.

230 Michaelmas

231 The surface roughness length was estimated at 1 cm, with an uncertainty range 0.01 -  
232 15 cm. Given the island conditions of high ground temperature and clear skies, the  
233 atmospheric stability condition was assumed to be very unstable (Monin-Obukhov  
234 Length ( $L$ ) = -10 m) and the variability in  $L$  was taken as:  $L_{max} = 100$  m to  $L_{min} = -5$   
235 m. The  $\text{NH}_3$  source area was assumed to be any part of the island that the birds were  
236 likely excrete on. The minimum this could have been was 6,000  $\text{m}^2$  but the best  
237 estimate used was 10,000  $\text{m}^2$ .

238 Ascension

239 The Monin-Obukhov length was estimated at -14.8 m using sonic anemometer data  
240 and ranged from 30 m to -5 m. The background  $\text{NH}_3$  concentration was measured at  
241  $0.1 \mu\text{g m}^{-3}$  with uncertainty ranging from  $0.02 \mu\text{g m}^{-3}$  to  $0.44 \mu\text{g m}^{-3}$  (Johnson, 1994).  
242 The  $\text{NH}_3$  source area was taken as any part of the island that the birds were likely to  
243 have excreted on, with a best estimate of 80,000  $\text{m}^2$  and uncertainty range from  
244 90,000  $\text{m}^2$  to 70,000  $\text{m}^2$ .

### 245 **3. Results**

#### 246 **3.1 Michaelmas Cay**

247 The  $\text{NH}_3$  concentrations measured at Michaelmas Cay during both sampling periods  
248 range between 35 – 72  $\mu\text{g m}^{-3}$  downwind of the colony (Supplementary Material  
249 Section 5). The upwind “background” level of 1.6 – 3.9  $\mu\text{g m}^{-3}$  is clearly impacted to  
250 some extent by the bird emissions and also somewhat higher than one would expect  
251 for a marine background, for example when compared with a minimum of  $0.01 \mu\text{g m}^{-3}$   
252 measured in the region (Quinn et al., 1990). The higher background may be caused  
253 by nearby seabirds (< 100m from bird colonies) or emissions from the three regularly  
254 visiting tourist vessels.

255 During the sampling periods local winds predominately came from the south east.  
256 This may place the sampling equipment downwind of the colony on occasion. Higher  
257 concentrations were measured at Masts 1 and 2 than at Mast 3. Low wind direction  
258 variability means that the source footprint sampled by ALPHA samplers was very  
259 near to being constant for the two measurement periods (Supplementary Material  
260 Section 5).

261 Scenarios were run in WindTrax to reflect variability in roughness length, which  
262 propagates a  $\pm 15\%$  uncertainty in the  $\text{NH}_3$  emission flux. Varying  $L$  ( $L_{max} = 100$  m to  
263  $L_{min} = -5$  m) resulted in  $\pm 29\%$  modelled  $\text{NH}_3$  emissions. The uncertainty in  
264 estimated  $\text{NH}_3$  emissions due to source area was  $\pm 13\%$ . Using the data of Quinn et al.  
265 (1990), background  $\text{NH}_3$  has minimal effect on the modelled emissions ( $\pm 2\%$ ).

266 The using the time-integrated passive  $\text{NH}_3$  measurement, the WindTrax modelling  
267 results show an average  $\text{NH}_3$  emission flux of  $21 \mu\text{g NH}_3 \text{ m}^{-2} \text{ s}^{-1}$  during Period 1 and  
268  $22 \mu\text{g NH}_3 \text{ m}^{-2} \text{ s}^{-1}$  during Period 2, respectively, from the colony on Michaelmas Cay  
269 (as summarized below in Table 1). There is a remarkable similarity between the  
270 measurement periods, where 23% lower  $\text{NH}_3$  concentrations in period 1, compared  
271 with period 2, were offset by higher wind speed, leading to only 5% lower  $\text{NH}_3$   
272 emissions. The overall uncertainty, on Michaelmas Cay using passive samplers, is  
273 estimated to be  $\pm 35\%$ , leading to an ammonia emission flux for the two periods of  
274  $21 \pm 8$  and  $22 \pm 8 \mu\text{g NH}_3 \text{ m}^{-2} \text{ s}^{-1}$ , respectively. Additional uncertainties related to the  
275 use of time-averaged  $\text{NH}_3$  concentrations are addressed in Section 4 below.

#### 276 **3.2 Ascension Island**

277 a) Passive Sampling Campaign Measurements

278 On Ascension Island the ALPHA samplers were exposed for 3 periods; the  
279 concentration and meteorological measurements are summarised in Supplementary  
280 Material Section 6. Upwind background concentrations were  $0.1 \mu\text{g m}^{-3}$  for all three  
281 periods. Ammonia concentrations decreased with distance away from the colony,  
282 particularly evident during Period 3 when the 5-point transect was used. The lowest  
283 concentrations were recorded during the second period and the highest during the  
284 third period. During the measurement period, the average atmosphere conditions were  
285 unstable, with the average Monin-Obukhov length equal to  $-15 \text{ m}$ , ranging from  $30 \text{ m}$   
286 to  $-5 \text{ m}$ .

287 Based on the time-integrated passive  $\text{NH}_3$  measurements, the calculated  $\text{NH}_3$   
288 emission fluxes for the three periods of the campaign were  $18, 5$  and  $29 \mu\text{g m}^{-2} \text{ s}^{-1}$ ,  
289 respectively (Table 1). The overall uncertainty of the  $\text{NH}_3$  emission estimate made  
290 using passive samplers on Ascension Island was estimated at  $\pm 24\%$ , with the largest  
291 uncertainties being area estimation and atmospheric conditions contributing  $7$  and  
292  $23\%$ , respectively (estimated using Method described in Section 2.3). The intra-period  
293 variability was much larger at  $\sim 70\%$ . These values are compared with the continuous  
294 estimates in Section 4.

295 <<INSERT TABLE 1>>

296 b) Continuous Sampling Campaign Measurements

297 Concentrations of  $\text{NH}_3$  were measured for 21 days and values over the range  $< 0.1$   
298 (limit of detection) -  $230 \mu\text{g m}^{-3}$  were observed (Figure 3 Upper panel). There was a  
299 strong diurnal cycle observable in the concentrations measured, with larger values  
300 during the day and smaller values at night. This corresponds to a very strong diurnal  
301 temperature cycle as demonstrated by the ground temperature measurements (Figure 3  
302 middle panel). Two large peaks in  $\text{NH}_3$  concentrations were observed at 0600 on  
303 25/05/10 and at 0800 on 06/06/10, corresponding to periods immediately after large  
304 rain events. There are five other peaks observable in the concentration time series and  
305 the reason for them is currently unknown.

306 <<INSERT FIGURE 3>>

307 The calculated ammonia emissions similarly show a strong diurnal pattern, with  
308 values increasing to a maximum during the hottest part of the day and decreasing to  
309 almost zero during the night (Figure 3). Ammonia emissions were largest after the  
310 rain event on the 6/6/10, with a maximum emission of  $377 \mu\text{g NH}_3 \text{ m}^2 \text{ s}^{-1}$ . In periods  
311 with no rain  $\text{NH}_3$  emissions were relatively small. The uncertainty in meteorological  
312 parameters and measurements were significantly lower in the active measurements.  
313 The key sources of error, as described above in Section 2.3 on passive sampling  
314 results, were the background  $\text{NH}_3$  concentrations and nesting area which resulted in  
315 an overall emission uncertainty of  $\pm 12\%$ .

316 Averaging for each hour of the day (Figure 4) shows the diurnal pattern with a high  
317 variability. An early afternoon maximum is seen (1300 - 1500) and night-time  
318 minimum (0000-0600). By integrating the average diurnal emission, as shown in  
319 Figure 4, the daily average  $\text{NH}_3$  emission for this campaign was estimated at  $1.6 \text{ g}$   
320  $\text{NH}_3 \text{ m}^{-2} \text{ day}^{-1}$  (or  $19 \mu\text{g m}^{-2} \text{ s}^{-1}$ ). The largest uncertainties and variability occurred  
321 during daytime emissions while the night-time variability was uniformly very low.

322 <<INSERT FIGURE 4>>



## 323 **4. Discussion**

### 324 **4.1 Comparison of passive time-integrated and continuous sampling campaigns**

325 Since making continuous measurements of NH<sub>3</sub> concentrations in remote locations is  
326 operationally much more challenging than making time-integrated passive  
327 measurements, the comparison of the two approaches for use in emission calculations  
328 is of high practical interest. In particular, using time averaged concentrations  
329 introduces additional errors associated with changing meteorological conditions, so  
330 that, subject to reliable NH<sub>3</sub> measurement, the continuous approach should be  
331 considered as the reference. Overall, the modelled NH<sub>3</sub> emission estimated using  
332 active and passive methods are very similar (Table 1), with the differences between  
333 chemical sampling strategies being smaller than the differences between sampling  
334 averaging periods. This is summarized in the last two columns of Table 1 which  
335 compare the Uncertainty associated with Sampling Period (USP) with the Uncertainty  
336 associated with Sampling Method (USM). These values are based on first making an  
337 additional estimate of the flux, based on averaging the NH<sub>3</sub> concentration data from  
338 the continuous on-line system to the same periods as for the passive NH<sub>3</sub>  
339 measurement (flux c). In this way, the difference between the continuous fluxes based  
340 on hourly data (flux a) and flux c represents USP, whereas the difference between the  
341 time integrated passive estimates (flux a) and flux c represents USM. The relative  
342 differences between flux a and flux b for the three periods on Ascension were: -18%, -  
343 44% and +4% (mean difference for the campaign: -12%). Thus, despite the additional  
344 errors induced by this practical simplification, passive sampling was found to generate  
345 valuable data when resources are not available for an active sampling campaign.

346 One reason why such close agreement was obtained between the different  
347 measurement strategies may be because most of the emissions from this source were  
348 associated with warm daytime unstable conditions, while cool nocturnal conditions  
349 were always associated with low emissions (Figure 2). In this way, errors associated  
350 with transition between meteorological conditions turned out to be relatively small in  
351 practice.

352 The similarity between the time-averaged emissions from active and passive sampling  
353 for all measurement periods shows that much of variability between the high  
354 resolution active sampling and the passive emissions are caused by differences in  
355 averaging period. Not only was the uncertainty of emission estimates resulting from  
356 the active campaign smaller, but the high resolution data collected by active sampling  
357 allowed for the observations of diurnal variations in NH<sub>3</sub> emission, showing the  
358 response of emission processes to dry and wet periods. Even though the active  
359 measurement method provides a great deal of data on NH<sub>3</sub> emission from seabird  
360 guano, it provides considerable logistical challenges, as the instruments are difficult to  
361 transport and require a power source. The passive campaigns are much more suited to  
362 measuring NH<sub>3</sub> concentrations at remote seabird colonies, especially if the objective  
363 is not to analyse processes in detail, but to estimate long-term or annual variations in  
364 NH<sub>3</sub> emission, similar to the study by Blackall et al. (2008). The advantages and  
365 disadvantages of the active and passive methods are shown in more detail in  
366 Supplementary Material Section 7.

### 367 **4.2 Weather conditions and environmental dependence of NH<sub>3</sub> emissions from** 368 **seabird colonies**

369 In order to understand the magnitude of NH<sub>3</sub> emissions and their effects on the  
370 environment, both the weather conditions and local environment are important. The  
371 present study estimated  $P_v$  ranging from 64% to 66% on Michaelmas Cay and from  
372 9% to 51% on Ascension Island (Table 1). According to the empirical temperature  
373 relationship investigated by Riddick et al. (2012), the  $P_v$  on both islands should be  
374 similar, given the similar surface temperature. Similarly, both islands are  
375 characterized by a ground environment with sandy/rocky surfaces and little  
376 vegetation, so that it is unlikely that substrate characteristics can explain the  
377 differences between the two sites.

378 The differences between the measured values of  $P_v$  can more easily be explained by  
379 the effect of rain events on ammonia emissions from the surface. During a rain event,  
380 water falling onto the relatively dry guano promotes bacterial hydrolysis of uric acid  
381 which is necessary for NH<sub>3</sub> emission to occur. On Michaelmas Cay, there were  
382 frequent rain events during the experiment, with average rainfall of around 4 mm day<sup>-1</sup>,  
383 while on Ascension Island there were only two significant rain events during the  
384 measurement campaign, with an average rainfall of 1 mm day<sup>-1</sup>. Both of the rain  
385 events on Ascension were followed by a significant increase in atmospheric NH<sub>3</sub>  
386 concentrations, consistent with increased uric acid hydrolysis following these events,  
387 with subsequent warm drying conditions promoting emissions (Figure 3). This was  
388 shown by much higher emissions during Periods 1 and 3, which had rain events,  
389 whereas Period 2 was rain free (Table 1).

390 While the larger precipitation rate at Michaelmas Cay allowed more rapid uric acid  
391 hydrolysis and larger  $P_v$  than at Ascension Island, it remains unclear whether even  
392 more rainfall at Michaelmas Cay would have further increased  $P_v$ . In principle, an  
393 optimum rate of water supply can be envisaged that will maximize NH<sub>3</sub> emissions:  
394 with too little water, uric acid hydrolysis becomes the limiting factor, while very wet  
395 conditions may promote N run-off, leaching and other loss processes (Blackall et al.,  
396 2008). In addition, wash-off by high tides may also deplete guano N pools at the  
397 colony. These factors imply that the initial temperature dependence estimated by  
398 Riddick et al. (2012) tends to overestimate NH<sub>3</sub> emissions in warm conditions, and  
399 that it is unlikely that  $P_v = 100%$  would occur frequently in real situations.

400 To assess these interactions of NH<sub>3</sub> emission with temperature, water availability and  
401 other losses more fully, the application of process-based modelling is required  
402 (Riddick, 2012; Sutton et al., 2013), which is the subject of on-going analysis, as well  
403 as measurements of emission rates in contrasting, sub-polar climates where major  
404 seabird colonies are located (Riddick, 2012). However, comparison of the present  
405 study with the published emission rates of Blackall et al. (2007) for temperate  
406 conditions already shows some differences. Blackall et al. (2007) estimated average  
407  $P_v$  at ~32% for bare rock breeders (Atlantic Gannet *Morus bassanus*, Bass Rock,  
408 Scotland), which is almost identical to the average  $P_v$  measured here for Ascension  
409 Island (31%). This suggests that the warmer conditions at Ascension (promoting  
410 increased  $P_v$ ) were substantially offset by water limitation. By contrast, at  
411 Michaelmas Cay, with less water limitation, warmer conditions than Scotland allowed  
412 a much larger fraction of the excreted guano N to volatilize as NH<sub>3</sub> (65%). By  
413 comparison, in sub-polar contexts, with temperatures around 0°C, Riddick (2012)  
414 estimated much smaller  $P_v$  (< 5%), highlighting the substantial sensitivity to weather  
415 of volatilization-based NH<sub>3</sub> emissions (Sutton et al., 2013). These model estimates are  
416 supported by the recent Antarctic measurement results of Theobald et al. (2013),  
417 showing how  $P_v$  appears to be much smaller under cold conditions.

## 418 **5. Conclusions**

419 In the analysis of both the continuous and passive measurement strategies,  
420 micrometeorological data and NH<sub>3</sub> concentrations were applied in an inverse  
421 Lagrangian dispersion model (WindTrax). In principle, non-stationarity leads to  
422 errors associated with long averaging periods, when calculating trace gas emissions in  
423 this way. By contrast, active, continuous measurements of NH<sub>3</sub> concentrations are  
424 operationally very challenging to conduct at remote locations. Our comparison of  
425 active and passive sampling strategies addressed this and showed that, in practice, the  
426 NH<sub>3</sub> emissions estimated at Ascension Island by both active and passive NH<sub>3</sub>  
427 concentration measurements were very similar. This provides some confidence in the  
428 higher estimated rate of volatilization at the Michaelmas Cay site, with this higher  
429 value attributed to higher water availability at this site.

430 The main advantage of high-resolution ammonia data is that it allows further  
431 understanding of the underlying processes in formation and subsequent NH<sub>3</sub> emission  
432 and how these processes are affected by climatic conditions such as temperature,  
433 precipitation, wind speed and relative humidity. Measured diurnal variations in NH<sub>3</sub>  
434 emissions emphasize the role that ground temperature plays, as emissions follow  
435 diurnal variation in ground temperature. The observations suggest NH<sub>3</sub> emissions  
436 were water-limited on Ascension, with higher water availability at Michaelmas Cay  
437 allowing larger  $P_v$ , despite similar temperatures at both sites.

438 The NH<sub>3</sub> concentrations measured on Ascension Island are similar to previous studies  
439 elsewhere. Based on passive sampling methods, maximum NH<sub>3</sub> weekly  
440 concentrations of 83  $\mu\text{g m}^{-3}$  were recorded at the Isle of May seabird colony that  
441 experience temperate weather conditions (Blackall et al., 2008), compared with 72  $\mu\text{g}$   
442  $\text{m}^{-3}$  at Ascension Island. In addition, the 15 minute continuous data at Ascension  
443 Island showed maximum peak concentrations of up 230  $\mu\text{g m}^{-3}$  at 100 m from the bird  
444 colony, as measured on the 06/06/10. These maximum NH<sub>3</sub> concentrations in air  
445 indicate potentially toxic environments near seabird colonies, and further studies are  
446 required to understand the impact of seabird nitrogen on local plant life.

447 The data presented in this paper give the first micrometeorological measurement-  
448 based NH<sub>3</sub> emission flux calculations for seabird colonies in tropical regions. The  
449 NH<sub>3</sub> emission measured on Michaelmas Cay showed that tropical seabird colonies  
450 can be significant sources of NH<sub>3</sub> emissions in remote areas. The largest tropical bird  
451 colonies are on Pacific Islands and remote islands in the Indian and Atlantic oceans,  
452 where bird colonies thrive in the absence of natural predators or anthropogenic  
453 disturbance. It is estimated that there are 116 tropical seabird colonies larger than the  
454 colony of 20,000 individual birds on Michaelmas Cay (Riddick et al., 2012). This  
455 study shows how seabird colonies create ammonia 'hotspots' that could affect the  
456 growth and structure of the local ecosystem, such as downwind dry shrub land on  
457 Ascension, as has been shown for many other N-limited ecosystems (Cape et al.,  
458 2009; Sutton et al., 2011). Of the several environmental factors affecting the rate of  
459 emission, ground temperature and water availability were found to be the most  
460 important, given similar temperature regimes.

## 461 **Acknowledgements**

462 This project was supported by a grant from the NERC CEH Integrating Fund and  
463 jointly carried out between the Centre for Ecology & Hydrology and King's College,  
464 London. Thanks to S. Stroud, N. Williams and O. Renshaw at the Conservation

465 Department on Ascension Island for providing permission and local support with this  
466 research. Thanks to J.C. Riddick for help in data capture.

467 Routine monthly surveys of seabird colonies on Michaelmas Cay were made within  
468 the framework of the seabird monitoring program through the joint Queensland Parks  
469 and Wildlife Service/Great Barrier Reef Marine Park Authority – Field Management  
470 Program undertaken by the Queensland Department of National Parks, Recreation,  
471 Sports and Racing.

## 472 **References**

473 Blackall, T.D., Theobald, M.R., Milford, C., Hargreaves, K.J., Nemitz, E., Wilson,  
474 L.J., Bull, J., Bacon, P.J., Hamer, K.C., Wanless, S. and Sutton, M.A. (2004)  
475 Application of tracer ratio and inverse dispersion methods with boat-based plume  
476 measurements to estimate ammonia emissions from seabird colonies. *Water, Air, &*  
477 *Soil Pollution: Focus*, 4, 279-285.

478 Blackall, T.D., Wilson, L.J., Theobald, M.R., Milford, C., Nemitz, E., Bull, J., Bacon,  
479 P.J., Hamer, K.C., Wanless, S. and Sutton, M.A. (2007) Ammonia emissions from  
480 seabird colonies. *Geophysical Research Letters*, 34, 5-17.

481 Blackall, T.D., Wilson, L.J., Bull, J., Theobald, M.R., Bacon, P.J., Hamer, K.C.,  
482 Wanless, S. and Sutton, M.A. (2008) Temporal variation in atmospheric ammonia  
483 concentrations above seabird colonies. *Atmospheric Environment*, 42, 6942-6950.

484 Cape, J.N., van der Eerden, L.J., Sheppard, L.J., Leith, I.D. and Sutton, M.A. (2009)  
485 Evidence for changing the Critical Level for ammonia. *Environmental Pollution*, 157,  
486 1033-1037.

487 ECN (2003) AiRRmonia. Energy Research Foundation of the Netherlands. Petten,  
488 NL. pp.57.

489 Elliott, H.A. and Collins, N.E. (1982) Factors affecting ammonia release in broiler  
490 houses. *Transactions of the ASAE*, 25, 413-418.

491 Ellis, J.C. (2005) Marine birds on land: a review of plant biomass, species richness,  
492 and community composition in seabird colonies. *Plant Ecology*, 181, 227-241.

493 EPA (2011) 40 Code of Federal Regulations Appendix B To Part 136 - Definition  
494 And Procedure For The Determination Of The Method Detection Limit-Revision  
495 1.11.

496 Flechard C.R., Massad R.-S., Loubet B., Personne E., Simpson D., Bash J.O., Cooter  
497 E.J., Nemitz E. and Sutton M.A. (2013) Advances in understanding, models and  
498 parameterisations of biosphere-atmosphere ammonia exchange. *Biogeosciences* **10**,  
499 5385-5497.

500 Flesch, T.K., Wilson, J.D. and Yee, E. (1995) Backward-time Lagrangian stochastic  
501 dispersion models, and their application to estimate gaseous emissions. *Journal of*  
502 *Applied Meteorology*, 34, 1320-1332.

503 Laubach, J., Kelliher, F.M., Knight, T.W., Clark, H., Molano, G. and Cavanagh, A.  
504 (2008) Methane emissions from beef cattle. *Australian Journal of Experimental*  
505 *Agriculture*, 48, 132-137.

506 Lindeboom, H.J. (1984) The nitrogen pathway in a penguin rookery. *Ecology*, 65,  
507 269-277.

508 NCDC (2011) National Climatic Data Center, Integrated Surface Hourly (ISH)  
509 database. <http://www.ncdc.noaa.gov/oa/climate/surfaceinventories.html> Downloaded  
510 Monday, 19-Dec-2011 04:44:15 EST. Accessed December 2011. URL was correct  
511 at a given date.

512 Nemitz, E., Milford, C. and Sutton, M.A. (2001) A two-layer canopy compensation  
513 point model for describing bi-directional biosphere-atmosphere exchange of  
514 ammonia. *Quarterly Journal of the Royal Meteorological Society*, 127, 815-833.

515 Norman, N. and Leck C. (2005), Distribution of marine boundary layer ammonia over  
516 the Atlantic and Indian Oceans during the Aerosols99 cruise, *Journal of Geophysical*  
517 *Research*, 110, D16302, doi:10.1029/2005JD005866.

518 NOAA (2010) National Oceanic and Atmospheric Administration - METAR Data  
519 Access. Accessed November 2011. URL was correct at a given date.  
520 <http://weather.noaa.gov/>

521 Norman, M., Spirig, C., Wolff, V., Trebs, I., Flechard, C., Wisthaler, A.,  
522 Schnitzhofer, R., Hansel, A. and Neftel, A. (2009) Intercomparison of ammonia  
523 measurement techniques at an intensively managed grassland site (Oensingen,  
524 Switzerland). *Atmospheric Chemistry*, 9, 2635-2645.

525 McGinn, S.M., Flesch, B.P., Crenna, T.K., Beauchemin, K.A. and Coates, T. (2007)  
526 Quantifying ammonia emissions from cattle feedlot using a dispersion model. *Journal*  
527 *of Environmental Quality*, 36, 1585-1590

528 Phillips, R.A., Thompson, D.R. and Hamer, K. C. (1999) The impact of Great skua  
529 predation on seabird populations at St Kilda: a bioenergetics model. *Journal of*  
530 *Applied Ecology*, 36, 218-232.

531 Puchalski, M.A., Sather, M.E., Walker, J.T., Lelunann, C.M.B., Gay, D.A., Mathew,  
532 J., Robarge, W.P., (2011). Passive ammonia monitoring in the United States:  
533 comparing three different sampling devices. *Journal of Environmental Monitoring* 13,  
534 3156-3167.

535 Quinn, P.K., Bates, T.S., Johnson, J.E., Covert, D.S. and Charlson, R.J. (1990),  
536 Interactions between the sulfur and reduced nitrogen cycles over the central Pacific  
537 Ocean, *Journal of Geophysical Research*, 95(D10), 16,405– 16,416.

538 Riddick, S.N. (2012) The global ammonia emission from seabirds. PhD thesis, King's  
539 College, London.

540 Riddick S.N., Dragosits U., Blackall T.D., Daunt F., Wanless S. and Sutton M.A.  
541 (2012) The global distribution of ammonia emissions from seabird colonies.  
542 *Atmospheric Environment*, 55, 312-327.

543 Schmidt, S., Mackintosh, K., Gillett, R., Pudmenzky, A., Allen, D.E., Rennenberg, H.  
544 and Mueller, J.F. (2010) Atmospheric concentrations of ammonia and nitrogen  
545 dioxide at a tropical coral cay with high seabird density. *Journal of Environmental*  
546 *Monitoring*, 12, 460-465.

547 Siefert, R.L., Scudlark J.R., Potter A.G., Simonsen A., and Savidge K.B. (2004)  
548 Characterization of atmospheric ammonia emissions from a commercial chicken  
549 house on the Delmarva Peninsula. *Environmental Science Technology*, 38, 2769-  
550 2778.

551 Sommer, S.G., McGinn, S.M. and Flesch, T.K. (2005) Simple use of the backwards  
552 Lagrangian stochastic dispersion technique for measuring emissions from small field  
553 plots. *European Journal of Agronomy*, 23, 1-7.

554 Sutton M.A., Miners B., Tang Y.S., Milford C., Wyers G.P., Duyzer J.H. and Fowler  
555 D. (2001) Comparison of low-cost measurement techniques for long-term monitoring  
556 of atmospheric ammonia. *Journal of Environmental Monitoring*, 3, 446-453.

557 Sutton M.A., Howard C.M., Erisman J.W., Billen G., Bleeker A., Grennfelt P., Van  
558 Grinsven H. and Grizzetti B. (Eds) (2011) *The European Nitrogen Assessment: Sources, Effects and Policy Perspectives*, Cambridge University Press.

560 Sutton, M., Reis, S., Riddick, S.N., Dragosits, U., Nemitz, E., Theobald, M.R., Tang,  
561 S., Braban, C.F., Vieno, M., Dore, A.J., Mitchell, R.F., Wanless, S., Daunt, F.,  
562 Fowler, D., Blackall, T., Milford, C., Flechard, C., Loubet, B., Massad, R.S., Cellier,  
563 P., Clarisse, L., van Damme, M., Ngadi, N., Clerbaux, C., Skj oth, C., Geels, C.,  
564 Hertel, O., Wichink Kruit, R.J., Pinder, R.W., Bash, J.O., Walker, J.D., Simpson, D.,  
565 Horvath, L., Misselbrook, T., Bleeker, A., Dentener, F., and de Vries, W.  
566 (2013) Towards a climate-dependent paradigm of ammonia emission and deposition.  
567 *Philosophical Transactions of the Royal Society B* 368 1621 20130166;  
568 doi:10.1098/rstb.2013.0166 1471-2970

569 Tang, Y.S., Cape, J.N. and Sutton, M.A. (2001) Development and types of passive  
570 samplers for NH<sub>3</sub> and NO<sub>x</sub>. In *Proceedings of the International Symposium on*  
571 *Passive Sampling of Gaseous Pollutants in Ecological Research*. The Scientific  
572 World, 1, 513-529.

573 Theobald, M.R., Crittenden, P.D., Hunt, A.P., Tang, Y.S., Dragosits, U. and Sutton,  
574 M.A. (2006) Ammonia emissions from a Cape fur seal colony, Cape Cross, Namibia.  
575 *Geophysical Research Letters*, 33, L03812.

576 Theobald M.R., Crittenden P.D., Tang Y.S. and Sutton M.A. (2013) The application  
577 of inverse-dispersion and gradient methods to estimate ammonia emissions from  
578 antarctic penguins. *Atmospheric Environment*, 81, 320-329.

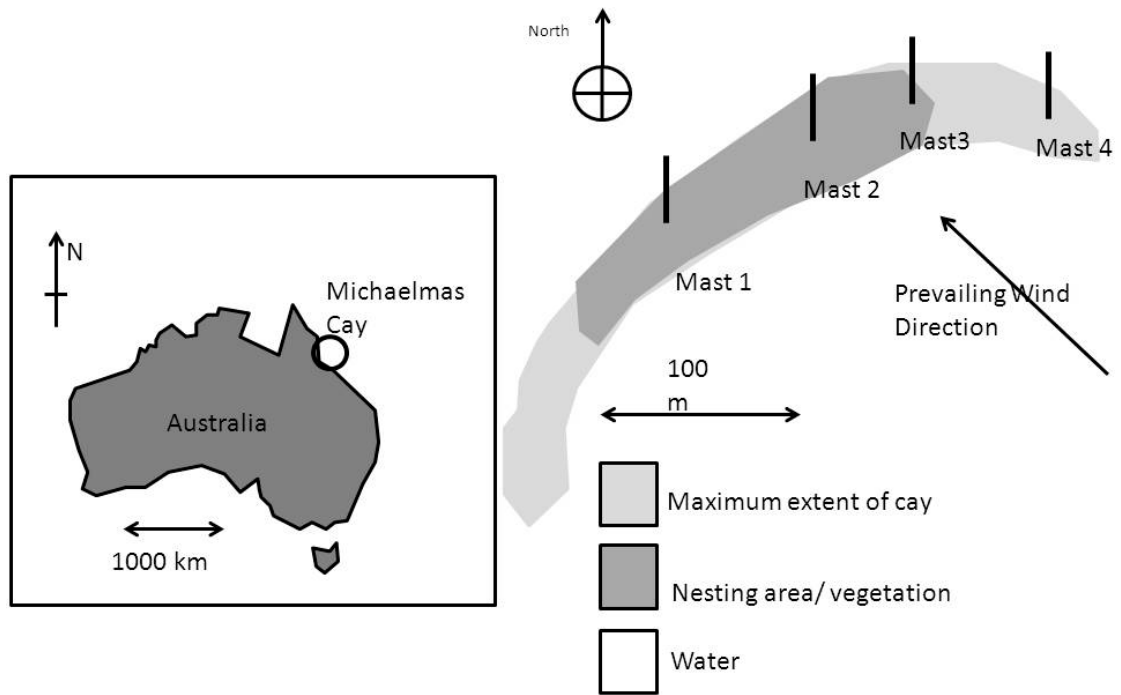
579 Vogt E., Dragosits U., Braban C.F., Theobald M.R., Dore A.J., van Dijk N., Tang  
580 Y.S., McDonald C., Murray S. and Sutton M.A. (2013) Heterogeneity of atmospheric  
581 ammonia at the landscape scale and consequences for environmental impact  
582 assessment. *Environmental Pollution* 179, 120-131. doi:10.1016/j.envpol.2013.04.014

583 Wilson, L.J., Bacon, P.J., Bull, J., Dragosits, U., Blackall, T.D., Dunn, T.E., Hamer,  
584 K.C., Sutton, M.A. and Wanless, S. (2004) Modelling the spatial distribution of  
585 ammonia emissions from seabirds in the UK. *Environmental Pollution*, 131, 173-185.

586 Wing, M.G., Eklund, A. and Kellogg, L.D. (2005) Consumer grade global positioning  
587 system (GPS) accuracy and reliability. *Journal of Forestry*, 103, 169-173.

588 Wright, P.A. (1995) Nitrogen excretion- 3 end-products, many physiological roles.  
589 *Journal of Experimental Biology*, 198, 273-281.

590

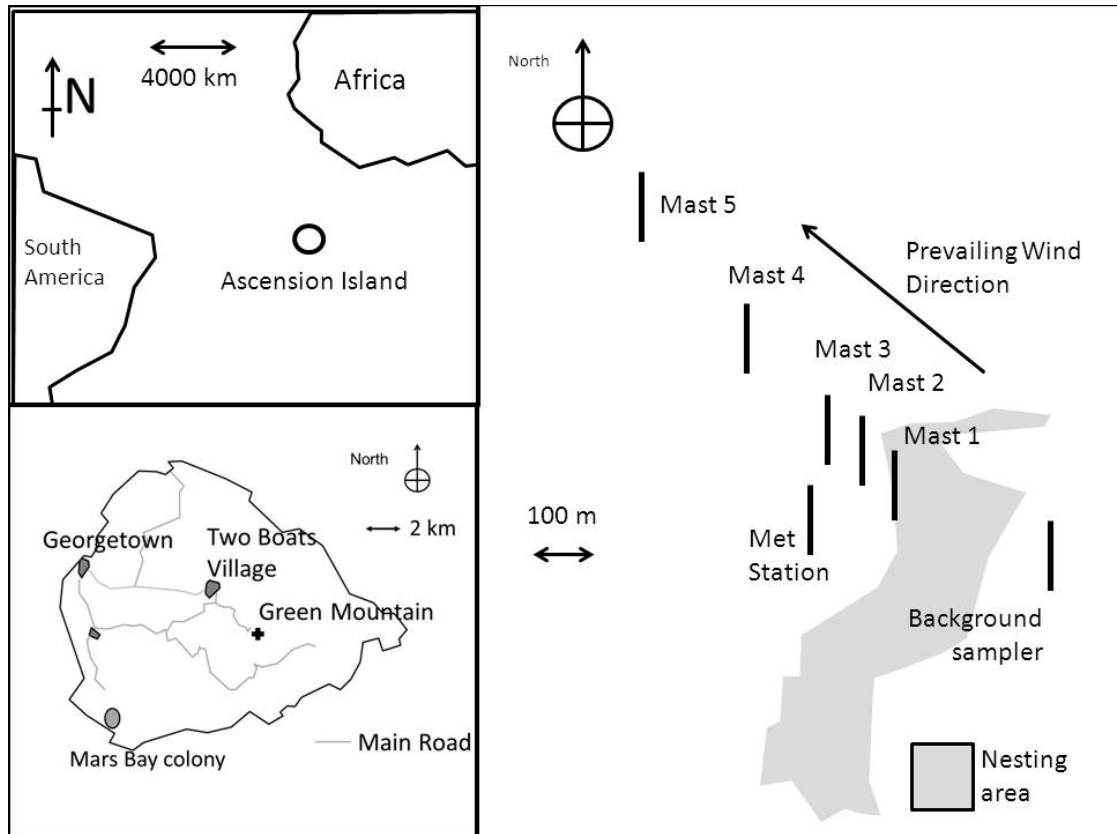


592

593 Figure 1 Location of ALPHA samplers on Michaelmas Cay. The birds nest on both  
 594 vegetation and sand. Map courtesy of Queensland Parks and Wildlife Service, Cairns,  
 595 Australia.

596

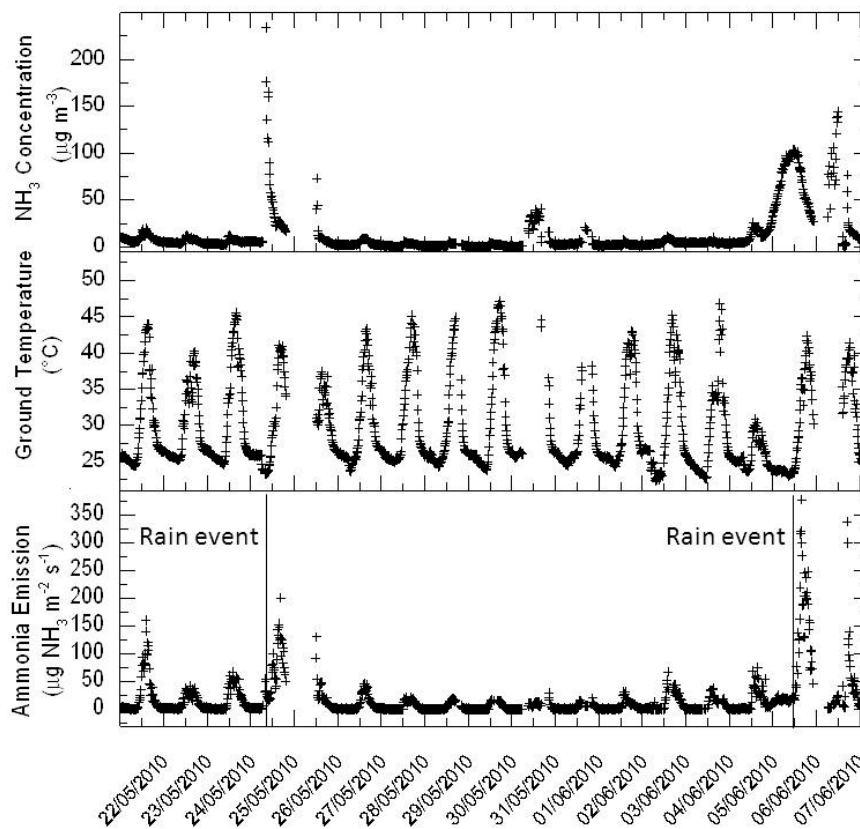
597  
598



599  
600  
601  
602  
603

Figure 2 Arrangement of ALPHA samplers used to measure the  $\text{NH}_3$  concentration at Mars Bay on Ascension Island. The “Source Area” indicates the extent of the Sooty terns’ nest site.





605

606

Figure 3 Time series of  $\text{NH}_3$  concentration, wind speed, ground temperature and

607

roughness length measured at Mars Bay, Ascension Island, 22/05/10 to 10/06/10.

608

These data were used as input to the WindTrax model for estimating  $\text{NH}_3$  emissions

609

from the seabird colony, shown at the bottom. Some data gaps are due to calibration

610

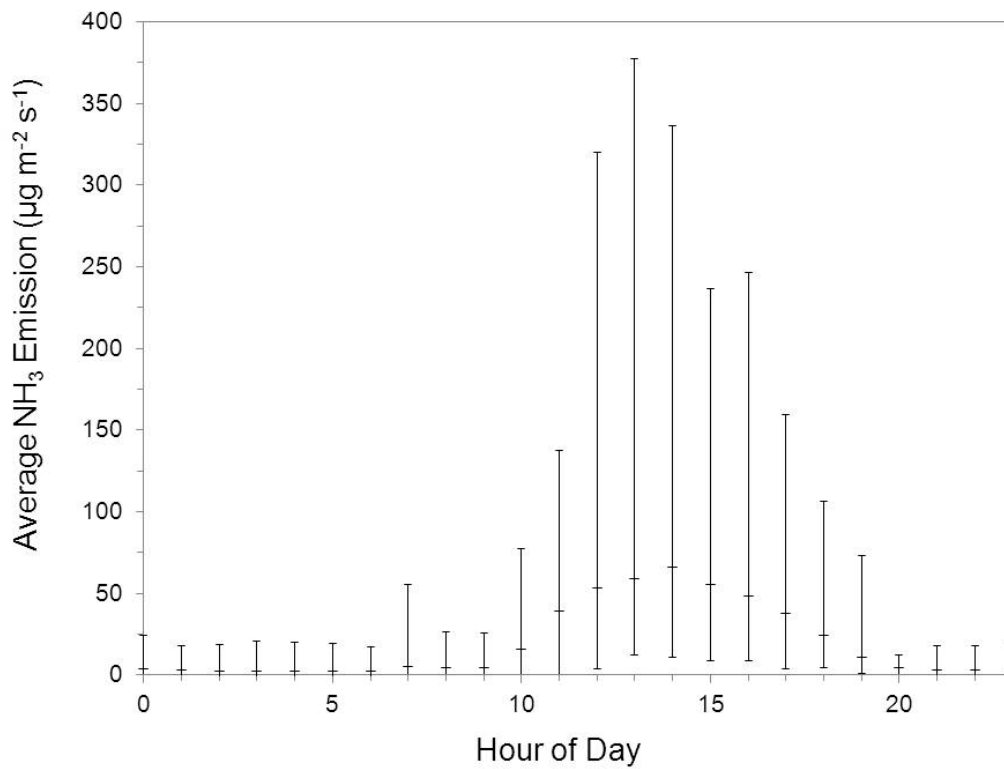
(21/05/10, 29/05/10 and 02/06/10). Also data gaps on 25/05/10 to 26/05/10 and

611

06/06/10 to 07/06/10 were periods where the instrument was not working.

612

613



615

616 Figure 4 Average diurnal pattern of NH<sub>3</sub> emissions derived from WindTrax emission  
617 calculations for the Sooty Tern colony at Mars Bay, Ascension Island. This campaign  
618 estimated an average daily NH<sub>3</sub> emission of 18.9 µg m<sup>-2</sup> s<sup>-1</sup> for the period 22/05/10  
619 and 10/06/10. The error bars show the variability in hourly emissions by representing  
620 the maximum and minimum NH<sub>3</sub> emissions for these hours for the duration of the  
621 campaign.

622

Colony	Measurement Period	Ground T(°C)	Rain (mm)	Passive		On-line measurement							
				Av. Flux NH <sub>3</sub> (µg m <sup>-2</sup> s <sup>-1</sup> ) (Flux a.)	P <sub>v</sub> (%)	Av. Flux NH <sub>3</sub> (µg m <sup>-2</sup> s <sup>-1</sup> ) (Flux b.)		Av. [NH <sub>3</sub> ] (µg m <sup>-3</sup> )		Flux using Av. [NH <sub>3</sub> ] (µg m <sup>-2</sup> s <sup>-1</sup> ) (Flux c.)		USP (µg m <sup>-2</sup> s <sup>-1</sup> )	US (µg m <sup>-2</sup> s <sup>-1</sup> )
1	1	30	5	21 ± 8	64								
1	2	32	106	22 ± 8	66								
2	1	30	5	18 ± 4	32	22 ± 3	37	13	20 ± 5	34	2	-2	
2	2	30	0	5 ± 1	9	9 ± 1	16	2	3 ± 1	5	6	2	
2	3	29	16	29 ± 7	51	28 ± 3	48	19	26 ± 6	45	2	3	

624

625 Table 1 Summary of seabird colony NH<sub>3</sub> emissions estimated from topical  
626 measurement campaigns. P<sub>v</sub> is the percentage of excreted nitrogen that volatilizes,  
627 Ground T is the ground temperature, USP represents the uncertainty in the flux  
628 attributable to the choice of sample averaging period and USM represents the  
629 uncertainty in the flux caused by the choice of sampling method (see notes below).  
630 Colony 1 indicates Michaelmas Cay and colony 2 indicates Ascension Island.

631

632

633 Supplementary Material Section 1

634 Tern and noddies' nesting area in the vegetation on Michaelmas Cay (photograph

635 courtesy of W. MacFarlane).



636  
637

638

639 Supplementary Material Section 2

640 Sooty terns nesting at the Mars Bay colony (photograph S. Riddick).



641  
642

643

644 Supplementary Material Section 3

645 Meteorological variables measured and derived during Ascension Island field  
646 campaign (\* indicates derived variable)

Variable	Instrument	Make	Units	Height (m)
Ground temperature	Tinytag Talk 2	Gemini Data Loggers, UK	°C	0
Rainfall	SBS500	Campbell Scientific, UK	mm	0
Air temperature	HMP45C Probe	Campbell Scientific, UK	°C	0.75
Relative Humidity	HMP45C Probe	Campbell Scientific, UK	%	0.75
Irradiance	SP Lite	Kipp & Zonen, NL	W m <sup>-2</sup>	0.75
Air pressure	CS100	Campbell Scientific, UK	Pa	0.75
Wind direction	Wind Sentry Vane	RM Young, USA	°	2
Wind speed	3-cup anemometers	RM Young, USA	m s <sup>-1</sup>	2
3D wind speed vectors	Windmaster Pro	Gill Instruments, UK	m s <sup>-1</sup>	2.5
Sonic temperature	Windmaster Pro	Gill Instruments, UK	°C	2.5
Monin-Obukhov length*	Windmaster Pro	Gill Instruments, UK	m	2.5
Friction velocity*	Windmaster Pro	Gill Instruments, UK	m s <sup>-1</sup>	2.5
Roughness length*	Windmaster Pro	Gill Instruments, UK	m	2.5

647

648

649

650

651 Supplementary Material Section 4

652 **Calculation of percentage of nitrogen volatilized ( $P_v$ )**

653 The percentage of nitrogen volatilized ( $P_v$ ) was calculated from the total nitrogen  
654 excreted at the colony during the measurement period and the total nitrogen  
655 volatilized as  $\text{NH}_3$ . The total nitrogen excreted ( $N$ ,  $\text{g N bird}^{-1} \text{ year}^{-1}$ ) is calculated  
656 using the bioenergetics model developed by Wilson et al. (2004) from bird specific  
657 data (Equation 1) and assumes that seabirds excrete N at a constant rate while at the  
658 colony. Bird specific data include; the adult mass ( $M$ ,  $\text{g bird}^{-1}$ ), nitrogen content of  
659 the food ( $F_{Nc}$ ,  $\text{g N g}^{-1}$  wet mass), energy content of the food ( $F_{Ec}$ ,  $\text{kJ g}^{-1}$  wet mass),  
660 assimilation efficiency of ingested food ( $A_{eff}$ ,  $\text{kJ [energy obtained] kJ}^{-1}$  [energy in  
661 food]), length of the breeding season ( $t_{breeding}$ , days), proportion of time spent at the  
662 colony during the breeding season ( $f_{tc}$ ). All values used in this study are taken from  
663 Riddick et al. (2012).

664 
$$N = \frac{9.2M^{0.774}}{F_{Ec}A_{eff}} F_{Nc} t_{breeding} f_{tc}$$
 Equation 1

665

666

667

668 Supplementary Material Section 5

669 Mean NH<sub>3</sub> concentrations ( $\mu\text{g m}^{-3}$ ) measured by ALPHA samplers on Michaelmas  
670 Cay during sampling periods and meteorological measurements used for modelling.671 The NH<sub>3</sub> concentrations show the mean (S.D.) of the three replicates measured by the

672 ALPHA samplers at each site.

Variable measure	Period 1	Period 2
Date of deployment	5/11/2009	10/12/2009
Date of retrieval	10/12/2009	6/1/2010
Mast 1 NH <sub>3</sub> concentration ( $\mu\text{g m}^{-3}$ )	55.3 (0.05)	70.7 (0.54)
Mast 2 NH <sub>3</sub> concentration ( $\mu\text{g m}^{-3}$ )	54.7 (1.36)	71.7 (0.06)
Mast 3 NH <sub>3</sub> concentration ( $\mu\text{g m}^{-3}$ )	37.7 (2.64)	35.4 (1.36)
Mast 4 NH <sub>3</sub> concentration ( $\mu\text{g m}^{-3}$ )	1.6 (0.04)	3.9 (0.02)
Ground temperature ( $^{\circ}\text{C}$ )**	29.7	32
Wind Speed ( $\text{m s}^{-1}$ )*	6.7	5.3
Wind Direction ( $^{\circ}$ to North)*	135 (28.9)	130 (64.5)
Total precipitation ( $\text{mm m}^{-2}$ )*	155	106
Roughness length (m)	0.01	0.01
Monin-Obukhov length, $L$ , (m)	-10	-10

\* NCDC (2011);

\*\* directly measured

673

674

675



676

677 Supplementary Material Section 6

678 Mean NH<sub>3</sub> concentration ( $\mu\text{g m}^{-3}$ ) measured by the ALPHA samplers deployed on  
 679 Ascension Island during the campaign and meteorological measurements. The NH<sub>3</sub>  
 680 concentrations show the mean (S.D.) of the three replicates measured by the ALPHA  
 681 samplers at each site.

Variable measure	Period 1	Period 2	Period 3
Date of deployment	20/05	27/05	02/06
Date of retrieval	27/05	02/06	09/06
Mast 1 NH <sub>3</sub> concentration ( $\mu\text{g m}^{-3}$ )	N/A	4.8 (0.58)	26.3 (0.18)
Mast 2 NH <sub>3</sub> concentration ( $\mu\text{g m}^{-3}$ )	N/A	2.4 (0.03)	13.4 (0.09)
Mast 3 NH <sub>3</sub> concentration ( $\mu\text{g m}^{-3}$ )	4.0 (0.08)	1.8 (0.03)	9.7 (0.01)
Mast 4 NH <sub>3</sub> concentration ( $\mu\text{g m}^{-3}$ )	2.2 (0.02)	N/A	3.6 (0.02)
Mast 5 NH <sub>3</sub> concentration ( $\mu\text{g m}^{-3}$ )	1.6 (0.08)	N/A	2.1 (0.10)
Background NH <sub>3</sub> concentration ( $\mu\text{g m}^{-3}$ )	0.1 (0.01)	0.1 (0.01)	0.1 (0.02)
Ground temperature ( $^{\circ}\text{C}$ )	30	30	28.8
Wind Speed ( $\text{m s}^{-1}$ )	5.1	4.9	4.7
Wind Direction ( $^{\circ}$ )	132	132	110
Total precipitation (mm)	5	0	16
Roughness length (m)	6.6	6.7	8.4
Monin-Obukhov length, $L$ , (m)	-12.7	-11.4	-21

682

683

684

685

686 Supplementary Material Section 7

687 Advantages and disadvantages of the active and passive sampling approach to estimate  
688 ammonia emissions from seabird colonies.

Method	Active	Passive
Advantages	<ol style="list-style-type: none"><li>1. Decreased uncertainty in the modelled meteorology when combining with continuous NH<sub>3</sub> concentrations.</li><li>2. Gives higher time resolution estimates of emissions for comparison with process models.</li></ol>	<ol style="list-style-type: none"><li>1. Operationally simpler to combine real time meteorology with time integrated NH<sub>3</sub> concentrations.</li><li>2. Can be implemented with much lower costs and using remote site operators, while allowing measurements at multiple locations.</li></ol>
Disadvantages.	<ol style="list-style-type: none"><li>1. Operationally much more challenging, including requirement for trained personnel to visit field site regularly to maintain semi-continuous NH<sub>3</sub> measurements.</li><li>2. Capital and personnel costs are much higher.</li><li>3. Significant electricity requirements for continuous NH<sub>3</sub> analyzers.</li><li>4. Gaps in data during instrument down-time and calibration.</li></ol>	<ol style="list-style-type: none"><li>1. Additional errors associated with averaging across changing meteorological conditions.</li><li>2. Only gives time averaged concentrations, according to sampling periods chosen.</li></ol>

689

690

691

692

693 Supplementary Material Section 8

694 The method detection limit (MDL) was calculated to the standards presented by the  
695 U.S. Environmental Protection Agency (EPA, 2011). The MDL was calculated using  
696 the following relationship:

697 
$$MDL = T_{(n-1, 1-\alpha=0.99)} \times SD$$

698 Where  $T_{(n-1, 1-\alpha=0.99)}$  is the t-value for the 99% confidence level and a standard  
699 deviation estimate with n - 1 degrees of freedom. The standard deviation (*SD*) is  
700 calculated from the number of blank samples (*n*) measured during each measurement  
701 campaign.

702